

## Kr Atoms and Their Clustering in Zeolite A

Woo Taik Lim,<sup>†</sup> Chang Hwan Chang,<sup>‡</sup> Kee Jin Jung, and Nam Ho Heo<sup>\*</sup>

<sup>†</sup>Pohang Accelerator Laboratory, Pohang University of Science and Technology,

P.O. Box 125, Pohang 790-600, Korea

<sup>‡</sup>Research Institute of Industrial Science and Technology, P.O. Box 125, Pohang 790-600, Korea

Department of Industrial Chemistry, Kyungpook National University, Taegu 702-701, Korea

Received April 16, 2001

The positions of Kr atoms encapsulated in the molecular-dimensioned cavities of fully dehydrated zeolite A of unit-cell composition  $\text{Cs}_3\text{Na}_8\text{HSi}_{12}\text{Al}_{12}\text{O}_{48}$  ( $\text{Cs}_3\text{-A}$ ) have been determined.  $\text{Cs}_3\text{-A}$  was exposed to 1025 atm of krypton gas at 400 °C for four days, followed by cooling at pressure to encapsulate Kr atoms. The resulting crystal structure of  $\text{Cs}_3\text{-A(6Kr)}$  ( $a = 12.247(2)$  Å,  $R_1 = 0.078$ , and  $R_2 = 0.085$ ) has been determined by single-crystal X-ray diffraction techniques in the cubic space group  $Pm\bar{3}m$  at 21(1) °C and 1 atm. In the crystal structure of  $\text{Cs}_3\text{-A(6Kr)}$ , six Kr atoms per unit cell are distributed over three crystallographically distinct positions: each unit cell contains one Kr atom at Kr(1) on a threefold axis in the sodalite unit, three at Kr(2) opposite four-rings in the large cavity, and two at Kr(3) on threefold axes in the large cavity. Relatively strong interactions of Kr atoms at Kr(1) and Kr(3) with  $\text{Na}^+$  ions of six-rings are observed:  $\text{Na-Kr(1)} = 3.6(1)$  Å and  $\text{Na-Kr(3)} = 3.08(5)$  Å. In each sodalite unit, one Kr atom at Kr(1) was displaced 0.74 Å from the center of the sodalite unit toward a  $\text{Na}^+$  ion, where it can be polarized by the electrostatic field of the zeolite, avoiding the center of the sodalite unit which by symmetry has no electrostatic field. In each large cavity, five Kr atoms were found, forming a trigonal-bipyramid arrangement with three Kr(2) atoms at equatorial positions and two Kr(3) atoms at axial positions. With various reasonable distances and angles, the existence of  $\text{Kr}_5$  cluster was proposed ( $\text{Kr(2)-Kr(3)} = 4.78(6)$  Å and  $\text{Kr(2)-Kr(2)} = 5.94(7)$  Å,  $\text{Kr(2)-Kr(3)-Kr(2)} = 76.9(3)$ ,  $\text{Kr(3)-Kr(2)-Kr(3)} = 88(1)$ , and  $\text{Kr(2)-Kr(2)-Kr(2)} = 60^\circ$ ). These arrangements of the encapsulated Kr atoms in the large cavity are stabilized by alternating dipoles induced on Kr(2) by four-ring oxygens and Kr(3) by six-ring  $\text{Na}^+$  ions, respectively.

**Keywords :** Zeolite A, Kr-Cluster, Nanocontainer.

### Introduction

Zeolites containing rare-gas atoms in their cavities are both ideal and realistic models for confined atoms.<sup>1-5</sup> Atoms confined in zeolitic cavities behave as finite fluids and not as subvolumes in independent equilibrium with an infinite reservoir.<sup>4,5</sup> A knowledge of the local structure adopted by such confined atoms is important in understanding the differences between the bulk and confinement-modified fluid properties, as they relate to transitions between phases, and to sorption and transport in such nanoporous materials.

Large quantities of gas molecules can be encapsulated in zeolite cavities if their molecular kinetic diameters are somewhat larger than the effective diameters of the zeolite windows. This can be accomplished by heating the zeolite and gas at high pressure, followed by quenching to ambient temperature while the high pressure is maintained.<sup>6-19</sup> These encapsulated gas molecules can sustain high-pressure concentration without leakage at room temperature; in this way zeolites may be used as storage media. Controlled decapsulation can be achieved by relaxing the window blockage by reheating the zeolite and/or by exposing the

zeolite to small polar molecules.<sup>16,20-22</sup> The utilization of zeolites as such a storage medium for small gas molecules was extensively examined, experimentally and theoretically, long ago by G. A. Cook,<sup>23</sup> D. W. Breck,<sup>24</sup> and R. M. Barrer *et al.*<sup>25-27</sup> In their work on argon (kinetic diameter = 3.40 Å) and krypton (3.60 Å), they concluded that these atoms must enter through six-ring windows of free diameter *ca.* 2.2 Å. It was subsequently shown that both cavities (the  $\alpha$ - and  $\beta$ -cages) of zeolite A can be utilized as nanocontainers for small gas molecules if all eight-ring windows are blocked by large monovalent cations such as  $\text{Cs}^+$ ,  $\text{Rb}^+$ , or  $\text{K}^+$ .<sup>9,10,11-13,28,29</sup>

Samant *et al.*<sup>30</sup> studied xenon atoms encapsulated in the  $\alpha$ -cages of Na-A as a storage medium at 525 K and 40 bar, resulting in up to 1.8 atoms per cage, by <sup>129</sup>Xe NMR. Their work showed that the <sup>129</sup>Xe chemical shift ( $\delta$ ) in a cavity smaller than the mean free path of xenon in the gas phase at the pressure of the experiment is a function of the size of the cavity and suggested that the peaks appearing at higher chemical shift correspond to an increasing number of xenon atoms per  $\alpha$ -cage. By studying the <sup>129</sup>Xe NMR spectrum of the sample saturated with water by exposure to excess water at room temperature, they showed that a xenon-water clathrate had formed, and suggested that the desorption of xenon from the zeolite upon water addition is probably due to solvation of the zeolitic cations, resulting in an opening of

<sup>\*</sup>Corresponding author. Tel: +82-53-950-5589; Fax: +82-53-950-6594; e-mail: nhheo@knu.ac.kr

the apertures to the  $\alpha$ -cages. Derouane and B'Nagy<sup>33</sup> related  $\delta_s$ , which is characterized as the specific physical interaction between sorbed xenon and the wall of the void space, with the surface curvature in calculating the physisorption energy. The sorbed xenon was required to remain near the surface in their model. Although the cage wall is theoretically the energetically most favorable position for sorption, direct experimental evidence for this was lacking. Dooryhee *et al.*<sup>31</sup> suggested, following synchrotron X-ray diffraction studies of Xe with Na-X at 31 °C at 1.0 and 1.75 atm, that the predominant site for Xe is in association with Na<sup>+</sup> ions in six-membered rings of the  $\alpha$ -cage. However, a molecular dynamics study by Santikary *et al.*<sup>32</sup> had concluded that the primary adsorption site is near the middle of a four-membered ring at the low loading of one Xe atom per  $\alpha$ -cage.

Heo *et al.*<sup>10</sup> extensively studied encapsulation capacities ( $V_{\text{gas}}$ ) of H<sub>2</sub>, N<sub>2</sub>, CO, CH<sub>4</sub>, and CO<sub>2</sub> for Cs<sub>2.5</sub>Na<sub>9.5</sub>-A (Cs-A) and Na<sub>12</sub>-A (Na-A) zeolites in order to understand the effect of molecular properties on the  $V_{\text{gas}}$ . Their calculation from the number of CO<sub>2</sub> molecules per unit cell, Heo *et al.* reported the density of encapsulated CO<sub>2</sub> (~18 wt%) in Cs-A approaches to 0.60 g/cm<sup>3</sup>, which is a value almost equal to that of liquid CO<sub>2</sub> (0.599) and much larger than that of saturated vapor at 30 °C (0.337). From these results, they postulated the presence of liquid-like phase for the encapsulated molecules in the molecular-dimensioned cavities of zeolite A. They also characterized Kr<sub>4</sub>, Ar<sub>4</sub>, Ar<sub>5</sub>, Xe<sub>2</sub>, Xe<sub>3</sub>, Xe<sub>4</sub>, and Xe<sub>5</sub> clusters, formed by confinement in the cavities of Cs<sub>3</sub>Na<sub>8</sub>H-A, by crystallographic studies.<sup>15,17,18</sup> In those structures of Cs<sub>3</sub>-A(5Ar), Cs<sub>3</sub>-A(5Kr), and Cs<sub>3</sub>-A(4.5Xe), four Ar, Kr, and Xe atoms in the large cavity formed a rhombus (planar) with an inter-inert gas atoms distance of 4.75(8), 4.67(3), and 4.51(3) Å and an angle of 88(1), 95.6(5), and 95.1(5)°, respectively. In this rhombic ring of four Ar, Kr, and Xe atoms, the charge dipoles induced on the Ar, Kr, and Xe atoms by their interactions with the zeolite alternate around the ring, showing the effect of the electrostatic fields in the zeolite cavity.<sup>15,17-19</sup> In the case of the structures of Cs<sub>3</sub>-A(6Ar)<sup>17</sup> and Cs<sub>3</sub>-A(5.25Xe),<sup>18</sup> the five Ar and Xe atoms in the large cavity have a trigonal-bipyramid arrangement with three Ar(2) and Xe(2) atoms at equatorial positions and two Ar(3) and Xe(3) atoms at axial positions with an inter-Ar and -Xe gas atoms distances of 4.63(9) and 4.45(2) Å. These arrangements of encapsulated Ar and Xe atoms in the large cavity are stabilized by alternating dipoles induced on Ar(2), Ar(3), Xe(2), and Xe(3) atoms by four-ring oxygens and six-ring Na<sup>+</sup> ions, respectively. Lim *et al.*<sup>19</sup> thoroughly studied Xe<sub>6</sub> cluster in the large cavity of native zeolite (Na<sub>12</sub>-A) by crystallographic method. In the structure of Na-A(7Xe), six Xe atoms in the large cavity formed a distorted octahedral arrangement with four Xe atom, at equatorial positions (each two at Xe(2) and Xe(3)) and the other two at axial positions (at Xe(4)). These arrangements of the encapsulated Xe atoms in the large cavity are also stabilized by alternating dipoles induced on Xe(2), Xe(3), and Xe(4) by eight- and six-ring Na<sup>+</sup> ions as well as four-ring oxygens, respectively.

In this work, Kr atoms, which are small gaseous atoms with high X-ray scattering power, have been encapsulated in the cavities of zeolite A at elevated temperature and much higher pressures (1025 atm of Kr gas) than previous work (635 atm of Kr gas).<sup>15</sup> Crystal structures of such zeolite encapsulate have been thoroughly studied for the understanding encapsulation characteristics of gas molecules, confinement effect, interactions between gas molecules and/or framework atoms of zeolite, and the possible clustering among the confined Kr atoms in the molecular-dimensioned cavities of zeolite A. The crystallographic results are important to elucidate the formation of interesting Kr clusters due to the induced dipolar attractions (London forces) in the large cavity as well as Kr atom trapped in the sodalite unit.

### Experimental Section

Colorless single crystals of zeolite 4A, Na<sub>12</sub>Si<sub>12</sub>Al<sub>12</sub>O<sub>48</sub>·27H<sub>2</sub>O (Na<sub>12</sub>-A·27H<sub>2</sub>O or Na-A·27H<sub>2</sub>O),<sup>34</sup> were synthesized by Kokotailo and Charnell.<sup>35</sup> Crystals of hydrated Cs<sub>3</sub>-A (approximate composition Cs<sub>3</sub>Na<sub>8</sub>H-A) were prepared by the dynamic (flow) ion-exchange of Na-A with an aqueous solution (pH = 5.7), 0.04 M in Cs<sup>+</sup> and 0.06 M in Na<sup>+</sup> made by using CsNO<sub>3</sub> and NaNO<sub>3</sub> (both Aldrich 99.99 %).<sup>14,15,17,18</sup> This solution composition was carefully chosen so that all eight- and six-ring sites of the zeolite would be fully occupied by Cs<sup>+</sup> and Na<sup>+</sup> ions with occupancies of 3.0 and 8.0 per unit cell, respectively.

A single crystal of hydrated Cs<sub>3</sub>-A, a cube 80 μm on an edge, was lodged in a fine Pyrex capillary with both ends open. This capillary was transferred to a high-pressure line connected to a vacuum line. After cautious increases in temperature of 25 °C/hr under vacuum, followed by complete dehydration at 400 °C and 1×10<sup>-4</sup> torr for two days, forced sorption of Kr into the crystal was carried out at 400 °C for four days with 1025 atm of Kr (Union Carbide, 99.999%). The high-pressure of Kr gas was produced by condensing the gas in a high-pressure chamber (immersed in a liquid-nitrogen bath) which contained the Cs<sub>3</sub>-A crystal in its capillary, followed by reheating to 400 °C after isolating the chamber from the vacuum line. Encapsulation was accomplished by cooling at pressure to room temperature with an electric fan. Following released of Kr gas from the chamber, both ends of the capillary were presealed with vacuum grease under nitrogen before being completely sealed with a small torch. No change was noted in the appearance of the crystal upon examination under the microscope.

The cubic space group  $Pm\bar{3}m$  (no systematic absences) was used in this work for reasons discussed previously.<sup>36,37</sup> For this crystal, the cell constant,  $a = 12.247(2)$  Å at 21(1) °C, was determined by a least-squares treatment of 15 intense reflections for which  $20 < 2\theta < 30^\circ$ . Each reflection was scanned at a constant scan speed of 0.5°/min in  $2\theta$  with a scan width of  $(0.42 + 0.46 \cdot \tan\theta)^\circ$ . Background intensity was counted at each end of a scan range for a time equal to half the scan time. The intensities of all lattice points for which  $2\theta < 70^\circ$

**Table 1.** Summary of Experimental and Crystallographic Data for Cs<sub>3</sub>Na<sub>8</sub>H-A(6Kr)

Ion exchange solutions	0.1 N 40 mol% (NaNO <sub>3</sub> + CsNO <sub>3</sub> )
Dehydration temperature	400 °C
Dehydration period	2 days
Encapsulation temperature	400 °C
Encapsulation pressure	1025 atm
Encapsulation period	4 days
No. of reflection obsd., <i>m</i>	134
No. of variables, <i>s</i>	36
Unit cell parameter	12.247(2) Å
Final error index	
<i>R</i> <sub>1</sub> <sup>a</sup>	0.078
<i>R</i> <sub>2</sub> <sup>b</sup>	0.085
Goodness-of-fit <sup>c</sup>	2.93

<sup>a</sup> $R_1 = \sum |F_o - |F_c|| / \sum F_o$ , <sup>b</sup> $R_2 = (\sum w(F_o - F_c)^2 / \sum w F_o^2)^{1/2}$ . <sup>c</sup>Goodness-of-fit =  $|\sum w(F_o - |F_c|)^2 / (m-s)|^{1/2}$

were recorded. Absorption corrections ( $\mu R$  ca. 0.27)<sup>38</sup> was judged to be negligible for this crystal since semi-empirical  $\psi$ -scans showed only negligible fluctuations for several reflections. Only those reflections in each final data set for which the net count exceeded three times its standard deviation were used in structure solution and refinement. This amounted to 134 reflections for the crystal. Other crystallographic details are the same as previously reported.<sup>15,17-19</sup> A summary of the experimental conditions and crystallographic data is presented in Table 1.

### Structure Determination

Full-matrix least-squares refinement was initiated with the atomic parameters of all framework atoms [(Si, Al), O(1), O(2), and O(3)], Cs<sup>+</sup> at Cs, and Na<sup>+</sup> at Na in Cs<sub>3</sub>Na<sub>8</sub>H-A.<sup>14</sup> The refinement with anisotropic thermal parameters for all atomic types in this model converged to the error indices  $R_1 = \sum |F_o - |F_c|| / \sum F_o = 0.196$  and  $R_2 = (\sum w(F_o - |F_c|)^2 / \sum w F_o^2)^{1/2} = 0.260$  with occupancies of 3.8(1) and 5.4(7) for Cs and Na, respectively. Introducing a Kr atom at a peak (0.3487,

0.3487, 0.3487, opposite six-ring) found in a difference Fourier function prepared from this model caused convergence to  $R_1 = 0.143$  and  $R_2 = 0.167$  in the following refinement with resulting occupancies of 3.21(7), 7.6(2), and 4.3(3) for Cs, Na, and Kr(3), respectively. Another difference Fourier function based on a model with fixed occupancies of 3.0 and 8.0 (their maximum values by symmetry) for Cs and Na, respectively, revealed a peak (0.3036, 0.3036, 0.5) opposite a four-ring in the large cavity. Including this peak as Kr atoms at Kr(2), the refinement converged to  $R_1 = 0.101$  and  $R_2 = 0.112$ , with resulting occupancies of 2.6(2) and 2.0(2) for isotropically refined Kr(2) and Kr(3), respectively. Addition of another peak (0.0504, 0.0504, 0.0504, inside the sodalite unit) at Kr(1) with an isotropic thermal parameter reduced the error indices to  $R_1 = 0.0836$  and  $R_2 = 0.0915$  with occupancies of 1.00(6), 2.8(3), and 2.0(2) for Kr(1), Kr(2), and Kr(3), respectively. Final cycles of refinement with occupancies fixed at 3.0, 8.0, 1.0, 3.0, and 2.0 for Cs, Na, and Kr(*i*), *i* = 1~3, respectively, converged to  $R_1 = 0.078$  and  $R_2 = 0.085$  with anisotropic thermal parameters. Again, extensive but unsuccessful efforts were made to locate the 12<sup>th</sup> cation necessary for electroneutrality at the usual position opposite a four-ring in the large cavity.<sup>14,15,17,18</sup> A final difference Fourier function was featureless; the notation Cs<sub>3</sub>-A(6Kr) or Cs<sub>3</sub>Na<sub>8</sub>H-A(6Kr) will be used for this crystal. All shifts in the final cycles of refinement were less than 0.1% for the corresponding estimated standard deviations. The final structural parameters are given in Table 2. Selected interatomic distances and angles are given in Table 3.

The values of the goodness-of-fit,  $(\sum w(F_o - |F_c|)^2 / (m-s))^{1/2}$ , are 2.93; the number of observations, *m*, is 134 and the number of parameters, *s*, is 36. The quantity minimized in least-squares is  $\sum w(F_o - |F_c|)^2$ , where the weights (*w*) are the reciprocal squares of  $\sigma(F_o)$ , the standard deviation of each observed structure factor. Atomic scattering factors for Kr, Na<sup>+</sup>, O<sup>-</sup>, and (Si,Al)<sup>1.75+</sup> were used. The function describing (Si,Al)<sup>1.75+</sup> is the mean of the Si<sup>4+</sup>, Si<sup>0</sup>, Al<sup>3+</sup>, and Al<sup>0</sup> functions. All scattering factors were modified to account for anomalous dispersion.<sup>39,40</sup>

**Table 2.** Positional, Thermal, and Occupancy Parameters<sup>a</sup>

Wyckoff position	x	y	z	<i>U</i> <sub>11</sub> or <i>U</i> <sub>iso</sub> <sup>b</sup>	<i>U</i> <sub>22</sub>	<i>U</i> <sub>33</sub>	<i>U</i> <sub>12</sub>	<i>U</i> <sub>13</sub>	<i>U</i> <sub>23</sub>	Occupancy <sup>c</sup>		
										fixed	varied	
(Si,Al)	24( <i>k</i> )	0	1839(7)	3713(7)	20(4)	17(4)	12(4)	0	0	0(5)	24 <sup>d</sup>	
O(1)	12( <i>h</i> )	0	2239(2)	5000 <sup>e</sup>	78(24)	17(16)	17(16)	0	0	0	12	
O(2)	12( <i>i</i> )	0	2948(2)	2948(2)	15(16)	48(13)	48(13)	0	0	24(18)	12	
O(3)	24( <i>m</i> )	1133(1)	1133(1)	3394(1)	33(8)	33(8)	51(15)	-1(11)	2(8)	2(8)	24	
Cs	3( <i>c</i> )	0	5000 <sup>e</sup>	5000 <sup>e</sup>	161(10)	56(3)	56(3)	0	0	0	3	3.21(7)
Na	8( <i>g</i> )	2028(15)	2028(15)	2028(15)	88(7)	88(7)	88(7)	76(9)	76(9)	76(9)	8	7.6(2)
Kr(1)	8( <i>g</i> )	349(38)	349(38)	349(38)	313(61)	313(61)	313(61)	-98(50)	-98(50)	-98(50)	1	1.00(6)
Kr(2)	12( <i>j</i> )	3003(24)	3003(24)	5000 <sup>e</sup>	195(25)	195(25)	372(62)	-103(37)	0	0	3	2.8(3)
Kr(3)	8( <i>g</i> )	3481(35)	3481(35)	3481(35)	366(49)	366(49)	366(49)	-5(55)	-5(55)	-5(55)	2	2.0(2)

<sup>a</sup>Positional parameters  $\times 10^4$  and thermal parameters  $\times 10^3$  are given. Numbers in parentheses are the estimated standard deviations in the units of the least significant figure given for the corresponding parameter. The anisotropic temperature factor is  $\exp[-2^2 a^2 (U_{11} h^2 + U_{22} k^2 + U_{33} l^2 + 2U_{12} hk + 2U_{13} hl + 2U_{23} kl)]$ . <sup>b</sup>Isotropic thermal parameters in units of Å<sup>2</sup>. <sup>c</sup>Occupancy factors are given as the number of atoms or ions per unit cell. <sup>d</sup>Occupancy for (Si) = 12, occupancy for (Al) = 12. <sup>e</sup>Exactly 0.5 by symmetry

**Table 3.** Selected Interatomic Distances (Å) and Angles (deg)<sup>a</sup>

Distances		Angles	
(Si,Al)-O(1)	1.649(2)	O(1)-(Si,Al)-O(2)	107.0(17)
(Si,Al)-O(2)	1.652(3)	O(1)-(Si,Al)-O(3)	112.4(7)
(Si,Al)-O(3)	1.687(2)	O(2)-(Si,Al)-O(3)	107.0(8)
Na-O(3)	2.27(3)	O(3)-(Si,Al)-O(3)	110.6(12)
Na-O(2)	2.96(2)	(Si,Al)-O(1)-(Si,Al)	146.2(27)
Cs-O(1)	3.39(4)	(Si,Al)-O(2)-(Si,Al)	157.8(20)
Cs-O(2)	3.53(3)	(Si,Al)-O(3)-(Si,Al)	143.3(7)
Kr(3)-Na	3.08(5)	O(3)-Na-O(3)	118.3(8)
Kr(1)-Na	3.6(1)	Kr(1)-Na-O(3)	82(2)
Kr(2)-Na	4.02(2)	Kr(3)-Na-O(3)	97.6(9)
Kr(2)-Cs	4.43(5)	Kr(1)-Na-Kr(3)	180 <sup>b</sup>
Kr(3)-Cs	5.01(7)	Kr(2)-Kr(3)-Kr(2)	76.9(3)
Kr(1)-O(3)	3.96(7)	Kr(3)-Kr(2)-Kr(3)	88(1)
Kr(1)-O(2)	4.5(2)	Kr(2)-Kr(2)-Kr(2)	60 <sup>c</sup>
Kr(2)-O(1)	3.83(2)		
Kr(2)-O(3)	3.81(4)		
Kr(3)-O(3)	3.98(6)		
Kr(3)-O(2)	4.28(1)		
Kr(2)-Kr(3)	4.78(6)		
Kr(2)-Kr(2)	5.94(7)		

<sup>a</sup>The numbers in parentheses are the estimated standard deviations in the units of the least significant digit given for the corresponding parameter.

<sup>b</sup>Exactly 180° by symmetry. <sup>c</sup>Exactly 60° by symmetry.

## Result and Discussion

**Zeolite A Framework and Cations.** The structural parameters of the framework atoms and cations are almost identical in all of the following structures: empty Cs<sub>3</sub>-A,<sup>14</sup> Cs<sub>3</sub>-A(5Ar),<sup>17</sup> Cs<sub>3</sub>-A(6Ar),<sup>17</sup> Cs<sub>3</sub>-A(5Kr),<sup>15</sup> and Cs<sub>3</sub>-A(xXe), x = 2.5, 4.5, and 5.25.<sup>18</sup> The occupancies of the Cs<sup>+</sup> ions in the eight-rings of the Kr encapsulate (Cs<sub>3</sub>-A(6Kr)) are slightly greater (closer to integral) than they were in empty Cs<sub>3</sub>-A<sup>14</sup> and Cs<sub>3</sub>-A(5Kr),<sup>15</sup> due to the (purposefully) higher Cs<sup>+</sup>/Na<sup>+</sup> ratio in the ion-exchange solution used for the preparation of Cs<sub>3</sub>-A in this work.

In the structure of Cs<sub>3</sub>-A(6Kr), three Cs<sup>+</sup> ions per unit cell fully occupy the centers of the eight-rings at equipoints of

**Table 4.** Deviations of Atoms (Å) from the (111) plane at O(3)<sup>a</sup>

Cs <sub>3</sub> -A(6Kr)	
Na	0.30
Kr(1)	-3.26 <sup>b</sup>
Kr(3)	3.38

<sup>a</sup>A negative deviation indicates that the atom lies on the same side of the plane as the origin, *i.e.*, inside the sodalite unit. <sup>b</sup>0.74 Å from the origin (center of the sodalite unit).

local symmetry  $C_{4h}$  ( $D_{4h}$  in  $Pm\bar{3}m$ ), positions commonly found in partially or fully Cs<sup>+</sup>-exchanged zeolite A.<sup>14,15,17-19,41-44</sup> Each Cs<sup>+</sup> ion is 3.39(4) Å from four O(1) oxygens and 3.53(3) Å from four O(2) oxygens (see Table 3). Although these distances are substantially longer than the sum, 2.99 Å, of the conventional ionic radii of O<sup>2-</sup> and Cs<sup>+</sup>, these positions are well established experimentally<sup>14,15,17-19,41-44</sup> and theoretically.<sup>45,46</sup>

As in the crystal structure of dehydrated Na<sub>12</sub>-A,<sup>47</sup> eight Na<sup>+</sup> ions per unit cell are located near the centers of the eight six-rings per unit cell. Each Na<sup>+</sup> ion is 2.27(3) Å from three O(3) oxygens (see Table 3 and Figure 2). These Na<sup>+</sup> ions extend 0.30 Å into the large cavity from the (111) planes at O(3) (see Table 4). The O(3)-Na-O(3) angles are close to 120° (118.3(8)°) showing that Na<sup>+</sup> is nearly trigonal, quite different from its near tetrahedral geometry in hydrated Cs<sub>3</sub>Na<sub>8</sub>H-A and Cs<sub>3</sub>Na<sub>9</sub>-A.<sup>14</sup> As in the previously reported crystal structure of the empty Cs<sub>3</sub>-A,<sup>14</sup> Cs<sub>3</sub>-A(5Ar),<sup>17</sup> Cs<sub>3</sub>-A(6Ar),<sup>17</sup> Cs<sub>3</sub>-A(5Kr),<sup>15</sup> and Cs<sub>3</sub>-A(xXe), x = 2.5, 4.5, and 5.25,<sup>18</sup> the 12<sup>th</sup> cation per unit cell, because it could not be located crystallographically, is assumed to be, at least predominantly, a H<sup>+</sup> ion. Alternatively, it may have been lost as water.<sup>14,15,17,18</sup>

**Krypton Atoms and Cluster in Cs<sub>3</sub>-A(6Kr).** Kr atoms in Cs<sub>3</sub>Na<sub>8</sub>H-A(6Kr) are found to populate most favorably at three crystallographically distinct positions. Each unit cell contains one Kr atom at Kr(1) on a threefold axis in the sodalite unit, three at Kr(2) opposite four-rings in the large cavity, and two at Kr(3) on threefold axes in the large cavity. The closest approach distances of these Kr atoms to the nonframework cations are 3.6(1) and 4.43(5) Å to Na<sup>+</sup> and Cs<sup>+</sup> ions, respectively, while that to framework oxygens is 3.81(4) Å (see Table 3). Considering the radii of the cations

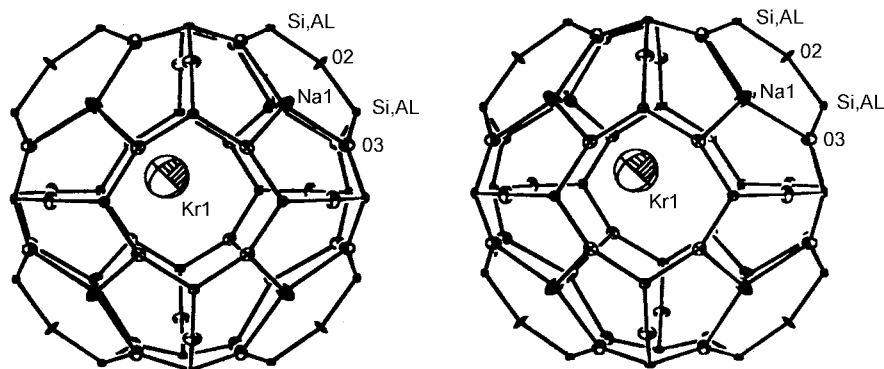


**Figure 1.** A stereoview of a sodalite unit in Cs<sub>3</sub>-A(6Kr), showing an encapsulated Kr atom near its center on a threefold axis. The zeolite A framework is drawn with light bonds between oxygens and tetrahedrally coordinated (Si,Al) atoms. Ellipsoids of 20% probability are shown.

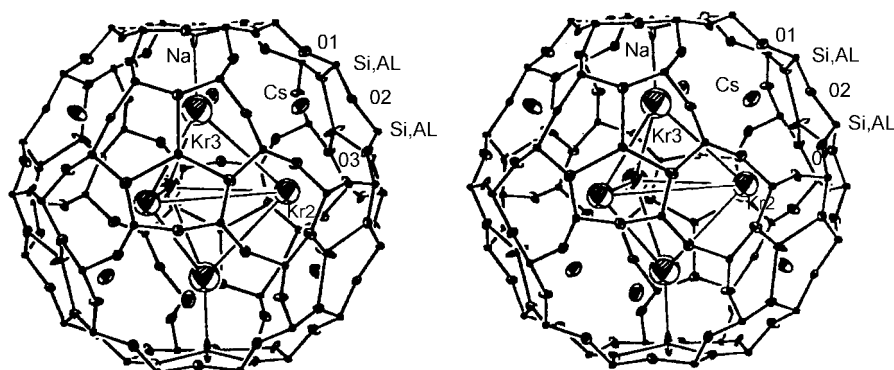


**Figure 2.** A stereoview of the large cavity of  $\text{Cs}_3\text{-A}(6\text{Kr})$  with the only reasonable (except for orientation) arrangement of three Kr atoms at Kr(2) and two at Kr(3). The five krypton atoms have a trigonal-bipyramid arrangement. See the caption to Figure 1 for other details.

( $r_{\text{Na}^+} = 0.97 \text{ \AA}$  and  $r_{\text{Cs}^+} = 1.67 \text{ \AA}$ ),<sup>49,50</sup> framework oxygens ( $1.32 \text{ \AA}$ ),<sup>49,50</sup> and Kr atoms ( $2.02 \text{ \AA}$  in solid Kr<sup>51</sup> and  $1.98 \text{ \AA}$  as  $r_{\text{min}}/2$ , half of the distance for maximum attraction from the Lennard-Jones potential<sup>48</sup>), all the Kr atoms are sufficiently far from their neighbors to be considered as having no more than weak interactions with the cations and framework oxygens. Similarly, inter-krypton distances of  $4.78(6) \text{ \AA}$  between Kr(2) and Kr(3) atoms, somewhat larger than those in solid Kr, are found in the large cavity.

**Kr Atom in the Sodalite Unit.** The location of an isolated Kr atom at Kr(1) on a threefold axis inside a sodalite unit is unambiguous (see Figure 1). It is impossible for some sodalite units to have zero Kr(1) atoms and others to have more than one at symmetry equivalent positions, to average to one, because impossibly short Kr(1)-Kr(1) distances would result. Therefore, every sodalite unit contains one ( $1.00(6)$ ) Kr(1) atom. A dynamic process for the passage of a Kr atom through a six-ring, whose aperture is formally too small, must exist at  $400^\circ\text{C}$  or at somewhat lower temperatures.

The closest approach of Kr(1) to a  $\text{Na}^+$  ion is  $3.6(1) \text{ \AA}$  and to three O(3) oxygens,  $3.96(7) \text{ \AA}$ . These approach distances are substantially longer than the sum of the atomic and ionic radii of Kr and  $\text{Na}^+$  ( $2.02 + 0.97 = 2.99 \text{ \AA}$ )<sup>49,51</sup> and the sum of those of Kr and  $\text{O}^{2-}$  ( $2.02 + 1.32 = 3.34 \text{ \AA}$ ),<sup>49,51</sup> respectively, indicating that Kr(1) is weakly held. Kr(1) is displaced  $0.74 \text{ \AA}$  from the center of the sodalite unit toward a  $\text{Na}^+$  ion, where it can be polarized by the electrostatic field of the zeolite, avoiding the center of the sodalite unit which by symmetry has no electrostatic field. Therefore, it can be concluded that there must be an attractive force between the polarized atom at Kr(1) and the electrostatic field of the zeolite with an energy minimum at this position.

This agrees qualitatively with a theoretical calculation for Kr in a sodalite-like cage.<sup>8</sup> The contours of constant London dispersion energy calculated in the presence of six-ring oxygens and  $\text{Na}^+$  ions showed a deep minimum at (0.1, 0.1, 0.1). Because the center of the sodalite cage was the position of minimum energy in similar calculations with no  $\text{Na}^+$  ions in the six-rings, this suggested an attractive force between Kr and a six-ring  $\text{Na}^+$  ion. Although the sodalite composition used in that work and that of  $\text{Cs}_3\text{-A}(6\text{Kr})$  are slightly different, the Kr(1) position in this structure indicates that

this Kr atom has its primary interaction with a  $\text{Na}^+$  ion.

**Kr Atoms in the Large Cavity.** The Kr atoms at Kr(3) are located on threefold axes in the large cavity, at positions similar to those found in the low temperature Kr sorption complex of  $\text{Ca}_4\text{Na}_4\text{-A}$ <sup>52</sup> and in the structure of  $\text{Cs}_3\text{-A}(5\text{Kr})$ <sup>15</sup> which was encapsulated at 635 atm of Kr gas. The approach distances of these Kr(3) atoms to six-ring  $\text{Na}^+$  ions,  $3.08(5) \text{ \AA}$ , are shorter than the corresponding Kr(1) distance,  $3.6(1) \text{ \AA}$ , as well as shorter than those found in the low temperature crystal structure of  $\text{Ca}_4\text{Na}_4\text{-A}(11\text{Kr})$ ,<sup>52</sup>  $3.48 \text{ \AA}$  (perhaps less accurate because powder data was used) and in the Kr encapsulate of  $\text{Cs}_3\text{-A}$ ,<sup>15</sup>  $3.23(2) \text{ \AA}$ . To approach  $\text{Na}^+$  ion, a Kr atom at Kr(1) must simultaneously approach three O(3) oxygens of the six-ring more closely than must an atom at Kr(3). This can be seen in the shorter Kr(1)-O(3) and Kr(3)-O(3) distances,  $3.96(7) \text{ \AA}$  and  $3.98(6) \text{ \AA}$ , respectively. These approaches may be repulsive at these short distances, and this may account for Kr(1)- $\text{Na}^+$ ,  $3.6(1) \text{ \AA}$ , being longer than Kr(3)- $\text{Na}^+$ ,  $3.08(5) \text{ \AA}$ . Alternatively, this may be described as being due to the stronger electrostatic field existing in the larger cavity, resulting in a shorter approach distance with stronger interactions between the polarized Kr atoms and  $\text{Na}^+$  ions. When the positions of  $\text{Na}^+$  and Kr atoms at Kr(3) is compared with that of  $\text{Cs}_3\text{-A}(5\text{Kr})$ , the  $\text{Na}^+$  ions at Na is slightly recessed into the center of the large cavity and Kr atoms at Kr(3) is lies on much closer position with the framework of the zeolite. These result in the shorter Kr(3)- $\text{Na}^+$ ,  $3.08(5) \text{ \AA}$ , and simultaneously longer Kr(2)-Kr(3),  $4.78(6) \text{ \AA}$ , as compared to Kr(3)- $\text{Na}^+$ ,  $3.23(2) \text{ \AA}$  and Kr(2)-Kr(3),  $4.67(3) \text{ \AA}$  in the structure of  $\text{Cs}_3\text{-A}(5\text{Kr})$ .<sup>15</sup> This is accounted as being due to the much stronger interactions between Kr atoms at Kr(3) and  $\text{Na}^+$  ions due to the much more population (“crowding”) of the Kr atoms in large cavity than in  $\text{Cs}_3\text{-A}(5\text{Kr})$ .<sup>15</sup> This is consistent with the study of dynamics of Xe atoms in NaA zeolites by Feng-Yin Li and R. Stephen Berry<sup>54</sup>, in which they suggested the contribution from Xe-Xe interaction becomes less important relative to the Xe-adsorption site of framework interaction even if the size of the Xe cluster increase to  $\text{Xe}_6$ .

Each of the three Kr(2) atoms, located opposite four-rings in the large cavity, approaches two O(1) oxygens and two O(3) oxygens with the same approach distances,  $3.83(2) \text{ \AA}$  and

3.81(4) Å, respectively. (Each Kr(2) must also interact with two Na<sup>+</sup> ions in adjacent six-rings with interatomic distances of 4.02(2) Å.) These distances are very similar to Kr(1)-O(3), 3.96(7) Å, and are the shortest Kr-O distances in the structure. These position of Kr atoms at Kr(2) and the approaching distance to framework oxygens are all identical with those of Cs<sub>3</sub>-A(5Kr)<sup>15</sup> except for the population (two Kr in Cs<sub>3</sub>-A(5Kr)<sup>15</sup> and three Kr in Cs<sub>3</sub>-A(6Kr)). This Kr(2) position is consistent with the results of Klinowski *et al.*,<sup>53</sup> which indicate that the four-ring is the most stable sorption site for xenon in dealuminated NaY.

The Kr-Na<sup>+</sup> interaction can be seen, on the basis of approach distances, to be somewhat stronger than the Kr-O (framework) interaction. If the conventional O<sup>2-</sup> radius (1.32 Å)<sup>49,50</sup> is subtracted from the average of the two Kr-O distances (3.82 Å), a “Kr interaction radius” of 2.50 Å is found. If the Na<sup>+</sup> radius (0.97 Å)<sup>49,50</sup> is subtracted from the mean (3.34 Å) of the Kr(1)-Na<sup>+</sup> and Kr(3)-Na<sup>+</sup> distances (3.6 and 3.08 Å, respectively), a smaller “Kr interaction radius”, 2.37 Å, is found. (These “Kr radii” can not be compared directly with those calculated and observed in solid Kr, 1.98<sup>48</sup> and 2.02 Å,<sup>51</sup> respectively.) This point may be made more simply but less reliably by noting that the mean Kr-Na<sup>+</sup> distance is 0.48 Å shorter than the mean Kr-O distance (3.82-3.34 = 0.48 Å).

**Clustering of Kr Atoms.** The five krypton atoms in the large cavity of Cs<sub>3</sub>-A(6Kr), three at Kr(2) and two at Kr(3), may also be placed within their partially occupied equipoints in various ways. The short distances among partially occupied equipoints of Kr(2) and Kr(3), such as 2.05(7) Å for Kr(2)-Kr(3) and 3.43(4) Å for Kr(2)-Kr(2), are impossibly short and are dismissed as before. The close inter-krypton interactions between equivalent krypton atoms (3.84(8) Å

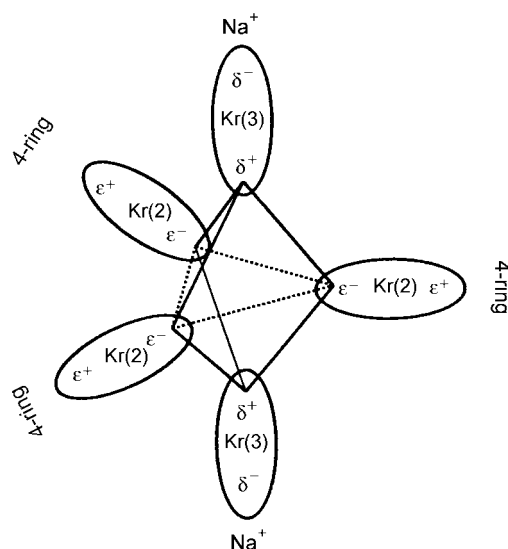


**Figure 3.** Schematic diagram of the trigonal bipyramid of five krypton atoms in the large cavities of Cs<sub>3</sub>-A(6Kr). The immediate environment of each Kr atom and the dipole moment in induces on each Kr are shown. The favorable interactions between the polarized Kr atoms are indicated by fine lines and the unfavorable ones by dashed lines.

for Kr(3)-Kr(3)) are dismissed because their induced dipoles are oriented unfavorably also as above. The next longest inter-krypton distance, 4.78(6) Å for Kr(2)-Kr(3) is plausible. However, various arrangements remain possible. A trigonal-bipyramid arrangement of those five Kr atoms as Kr<sub>5</sub> is selected as most plausible because of its higher symmetry and by considerations regarding alternating polarizations krypton atoms as before with Cs<sub>3</sub>-A(6Ar),<sup>17</sup> Cs<sub>3</sub>-A(5.25Xe)<sup>18</sup> (see Figures 2 and 3). Two Kr(3) atoms of the Kr<sub>5</sub> cluster on a single threefold axis opposite sides of the large cavity occupy axial positions and the other three Kr(2) atoms are at equatorial positions with inter-krypton distances of 4.78(6) Å for Kr(2)-Kr(3) and 5.94(7) Å for Kr(2)-Kr(2). In this arrangement, ε<sup>-</sup> polarizations from all three Kr(2) atoms point toward the center of the large cavity where each can interact with each of the two δ<sup>+</sup> polarizations from the threefold-axis Kr(3) atoms (see Figure 3). The favorable Kr(2)-Kr(3) interactions, 4.78(6) Å, are nicely much shorter than the unfavorable equatorial Kr(2)-Kr(2) interactions, 5.94(7) Å.

**Acknowledgment.** W. T. Lim gratefully acknowledges the post-doctoral fellowship of PAL (Pohang Accelerator Laboratory). We also gratefully acknowledge the support of the Central Laboratory of Kyungpook National University for the diffractometer and computing facilities.

**Supplementary Material Available:** Observed and calculated structure factors for Cs<sub>3</sub>-A(6Kr) are available upon request to the corresponding author.

## References

- Guemez, J.; Velasco, S. *Am. J. Phys.* **1987**, *55*, 154-157.
- Woods, G. B.; Rowlinson, J. S. *J. Chem. Soc., Faraday Trans. 2* **1989**, *85*, 765-781.
- Cooper, D. W. *Phys. Rev. A* **1988**, *38*, 522-524.
- Chmelka, B. F.; Raftery, D.; McCormick, A. V.; de Menorval, L. C.; Levine, R. D.; Pines, A. *Phys. Rev. Lett.* **1991**, *66*, 580-583.
- McCormick, A. V.; Chmelka, B. F. *Molecular Physics* **1991**, *73*, 603-617.
- Breck, D. W. *Zeolite Molecular Sieve: Structure, Chemistry, and Uses*; John Wiley & Sons: New York, 1974; pp 623-628.
- Fraenkel, D. *CHEMTECH* **1981**, *1*, 60-65.
- Barrer, R. M.; Vaughan, D. E. W. *J. Phys. Chem. Solids* **1971**, *32*, 731-743.
- Fraenkel, D.; Shabtai, J. *J. Am. Chem. Soc.* **1977**, *99*, 7074-7076.
- Kwon, J. H.; Cho, K. H.; Kim, H. W.; Suh, S. H.; Heo, N. H. *Bull. Korean Chem. Soc.* **1993**, *14*, 583-588.
- Yoon, J. H.; Heo, N. H. *J. Phys. Chem.* **1992**, *96*, 4997-5000.
- Heo, N. H.; Rho, B. R.; Kim, D. H.; Kim, J. T. *Hwahak Konghak* **1991**, *29*, 407-416.
- Kim, D. H.; Kim, J. T.; Heo, N. H. *Hwahak Konghak* **1991**, *29*, 717-726.
- Cho, K. H.; Kwon, J. H.; Kim, H. W.; Park, C. S.; Heo, N. H. *Bull. Korean Chem. Soc.* **1994**, *15*, 297-304.
- Heo, N. H.; Cho, K. H.; Kim, J. T.; Seff, K. *J. Phys. Chem.*

- 1994, 98, 13328-13333.
16. Kwon, J. H., M. E. Thesis; Kyungpook National University: 1993.
17. Heo, N. H.; Lim, W. T.; Seff, K. *J. Phys. Chem.* **1996**, 100, 13725-13731.
18. Heo, N. H.; Lim, W. T.; Kim, B. J.; Lee, S. Y.; Kim, M. C.; Seff, K. *J. Phys. Chem. B* **1999**, 103, 1881-1889.
19. Lim, W. T.; Park, M.; Heo, N. H., *Bull. Korean Chem. Soc.* **2000**, 21, 75-80.
20. Barrer, R. M.; Vansant, E. F.; Peeters, G. *J. Chem. Soc., Faraday Trans. I* **1978**, 74, 1871-1881.
21. Thijs, A.; Peeters, G.; Vansant, E. F.; Verhaert, I. *J. Chem. Soc., Faraday Trans. I* **1986**, 82, 963-975.
22. Niwa, M.; Kato, S.; Hattori, T.; Marakami, Y. *J. Chem. Soc., Faraday Trans. I* **1984**, 80, 3135-3145.
23. Cook, G. A. *Argon, Helium, and the Rare Gases*; Interscience: New York: **1961**; 1, Vol. 1, p 228.
24. Breck, D. W. *J. Chem. Educ.* **1964**, 41, 678-689.
25. Barrer, R. M.; Gibbons, R. M. *Trans. Faraday Soc.* **1963**, 59, 2569-2582.
26. Barrer, R. M.; Vaughan, D. E. W. *Trans. Faraday Soc.* **1967**, 63, 2275-2290.
27. Barrer, R. M.; Vaughan, D. E. W. *Surf. Sci.* **1969**, 14, 77-92.
28. Fraenkel, D. *J. Chem. Soc., Faraday Trans. I* **1981**, 77, 2029-2039.
29. Fraenkel, D.; Ittah, B.; Levy, M. *J. Chem. Soc., Chem. Commun.* **1984**, 1391-1392.
30. Samant, M. G.; de Menorval, L. C.; Dalla Betta, R. A.; Boudart, M. *J. Phys. Chem.* **1988**, 92, 3937-3938.
31. Dooryhee, E.; Greaves, G. N.; Steel, A. T.; Townsend, R. P.; Carr, S. W.; Thomas, J. M.; Catlow, C. R. A. *Faraday Discuss. Chem. Soc.* **1990**, 89, 119-136.
32. Santikary, P.; Yashonath, S.; Ananthakrishna, G. *J. Phys. Chem.* **1992**, 96, 10469-10477.
33. Derouane, E. G.; Nagy, J. B. *Chem. Phys. Lett.* **1987**, 137, 341-344.
34. The nomenclature refers to the contents of the  $Pm\bar{3}m$  unit cell: e.g., Na<sub>12</sub>-A represents Na<sub>12</sub>Si<sub>12</sub>Al<sub>12</sub>O<sub>48</sub>.
35. Charnell, J. F. *J. Crystal Growth* **1971**, 8, 291-294.
36. Cruz, W. V.; Leung, P. C. W.; Seff, K. *J. Am. Chem. Soc.* **1978**, 100, 6997-7003.
37. Mellum, M. D.; Seff, K. *J. Phys. Chem.* **1984**, 88, 3560-3563.
38. *International Tables for X-ray Crystallography*; Kynoch Press: Birmingham, England, 1974; Vol IV, pp 61-66.
39. Cromer, D. T. *Acta Crystallogr.* **1965**, 18, 17-23.
40. *International Tables for X-ray Crystallography*; Kynoch Press: Birmingham, England, 1974; Vol IV, pp 148-150.
41. Heo, N. H.; Seff, K. *J. Am. Chem. Soc.* **1987**, 109, 7986-7992.
42. Vance, T. B., Jr.; Seff, K. *J. Phys. Chem.* **1975**, 79, 2163-2167.
43. Firor, R. L.; Seff, K. *J. Am. Chem. Soc.* **1977**, 99, 6249-6253.
44. Subramanian, V.; Seff, K. *J. Phys. Chem.* **1979**, 83, 2166-2169.
45. Ogawa, K.; Nitta, M.; Aomura, K. *J. Phys. Chem.* **1978**, 82, 1655-1660.
46. Takaishi, T.; Hosoi, H. *J. Phys. Chem.* **1982**, 86, 2089-2094.
47. Yanagida, R. Y.; Amaro, A. A.; Seff, K. *J. Phys. Chem.* **1973**, 77, 805.
48. Breck, D. W. *Zeolite Molecular Sieve: Structure, Chemistry, and Uses*; John Wiley & Sons: New York, 1974; pp 634-641.
49. *Handbook of Chemistry and Physics*, 64<sup>th</sup> ed.; Chemical Rubber Co.: Cleveland, OH, 1983; pp F-187.
50. Shannon, R. D.; Prewitt, C. T. *Acta Crystallogr., Sect. B* **1969**, 25, 925-946.
51. Figgins, B. F.; Smith, B. L. *Philos. Mag.* **1960**, 5, 186-188.
52. Seff, K., *Ph. D. Thesis*; M.I.T.: 1964 and references therein.
53. Anderson, M. W.; Klinowski, J.; Thomas, J. M. *J. Chem. Soc., Faraday Trans. I* **1986**, 82, 2851-2862.
54. Li, F. Y.; Berry, S. R. *J. Phys. Chem.* **1995**, 99, 2459-2468.
-